ANISOTROPIC, ELASTIC-PLASTIC-THERMAL STRESS ANALYSES OF SOLID STRUCTURES

F.C. WEILER*

Aerotherm Corporation, Mountain View, California, U.S.A.

ABSTRACT

The anisotropic, elastic-plastic-thermal response of solid structures is described. First, anisotropic, thermal plasticity theory is reviewed followed by several numerical examples to indicate the importance of a correct material description. The last section explores the behavior of mechanically and thermally loaded nuclear grade graphites (typical of an environment in the core of a reactor) to ascertain the elastic-plastic-thermal response of graphite under these conditions.

An anisotropic thermal-plasticity theory is presented, including the three-dimensional yield surface in stress space and the appropriate associated thermal-plastic flow law based upon a set of restrictive conditions. Appropriate inclusion of the temperature dependence of the yield surface, and the resulting terms in the plastic flow law is shown. The final form of both the anisotropic thermal-elastic and thermal-plastic incremental constitutive equations are then described for use with the finite element method of solution. The incremental tangent-stiffness approach is described.

The importance of a correct orthotropic material description is shown by two numerical examples of thermally loaded hollow, plane strain cylinders. The first example compares solutions with different yield stresses in the hoop direction to ascertain its importance. The second example compares solutions of the same problem solved two different ways; including the temperature rate terms and neglecting them.

The orthotropic, temperature dependent behavior of graphite is demonstrated by descriptions of their mechanical properties. The first example problem is composed of graphite ATJ-S, and loaded by a thermal gradient. Comparisons are given for solving this problem by both the direct iterative method (deformational plasticity theory) and the incremental method (incremental plasticity theory). The second example problem compares the differences in the stress and strain states for two solutions which differ only in the method of the graphite material property descriptions. In the first solution, the actual stress-strain curves are used whereas in the second solution, a best fit least squares bi-linear form of the stress-strain curves are used. The results of these graphite studies are summarized and further areas of exploration of anisotropic, thermal plasticity are indicated.

* at present: Weiler research, Inc., Sunnyvale, California, U.S.A.

Predicting the inelastic thermostructural response of graphites is a difficult task due to the unusual behavior it exhibits under thermal and mechanical loading. At room temperatures, graphites such as ATJ-S and Graphitite G-90 deform in tension by a tearing mechanism which tends to elongate micro pores or voids. In compression, these voids are compressed and the tearing mechanism doesn't seem to be present. When examining the uniaxial stress-strain curves, the response in most of the temperature range of interest resembles that of a typical elastic-plastic material (ignoring visco elastic or visco plastic considerations for the present), that is, a definite elastic response portion of the curve seems to exist. Experimenters [Ref. 1] have noticed that by loading to some intermediate stress level, followed by unloading, no appreciable permanent strains were present. However, after loading to higher stress levels followed by unloading, permanent inelastic strains started to appear. This phenomenon may therefore be modeled on a macroscopic scale as an elastic-plastic response and such is the intent of this paper. For loading conditions of interest to the author, the strain rates are moderate (around 10^{-2} in/in sec) and times at load small (less than a few minutes) and consequently visco elastic-plastic effects are not present and will not be considered. It is the aim of the present paper to construct and use a mathematical theory which will describe the elastic-plastic-thermal response based upon input data which is currently available for the graphites in question. Admittedly, higher order theories would more closely represent the response, however, additional complicated testing (usually biaxial or triaxial types of tests) would be required to drive the necessary material parameters. With this view in mind, the following incremental elastic-plastic-thermal constitutive equations were derived.

Yield Functions or Yield Surfaces

All consistent incremental theories of plasticity are closely linked with the concept of yield functions or yield surfaces which determine whether or not, for some given set of stress increments, further plastic deformation will take place. In general, values and forms of the yield function will depend upon the state variables, e.g., stress, plastic strain, temperature, plastic work, etc.

The yield function postulated here was first introduced by Hill [Ref. 2] and later by Hu and Marin [Ref. 3], i.e.,

$$f = \bar{\sigma}^2 - \bar{y}^2 = 0 \tag{1}$$

where $\bar{\sigma}$, $\bar{y}$ are the equivalent stress and equivalent yield stress and f the yield function. The equivalent stress $\bar{\sigma}$ is defined in cylindrical coordinates for axisymmetric loading by

$$\bar{\sigma}^2 = \alpha_{r\theta}(\sigma_r - \sigma_\theta)^2 + \alpha_{\theta z}(\sigma_\theta - \sigma_z)^2 + \alpha_{zr}(\sigma_z - \sigma_r)^2 + \beta_{rz}\sigma_{rz}^2 \tag{2}$$

Originally, Hill, Hu and Marin assumed that the α anisotropy parameters were constants, determined by the initial yield stress in the principal material directions. However, for strain hardening materials they should not be constants. The objective is to determine the variation in the α parameters in such a manner that all of the stress-strain diagrams in the principal material directions are correctly reproduced when "mapped" on to an equivalent stress ($\bar{\sigma}$) - equivalent strain ($\bar{\epsilon}$) diagram. A particularly attractive method of accomplishing this mapping is given by Jensen, Falby and Prince [Ref. 4].

This is done based on the assumption that the anisotropic parameters (α) are determined such that, for equal amounts of plastic work done during stress-strain tests in all the principal directions, the effective stress level $\bar{\sigma}$ reached will be the same. The details of the method for obtaining the anisotropic parameters are given in Ref. 5. When the stress-strain diagrams may be expressed in bi-linear form as shown in Fig. 1

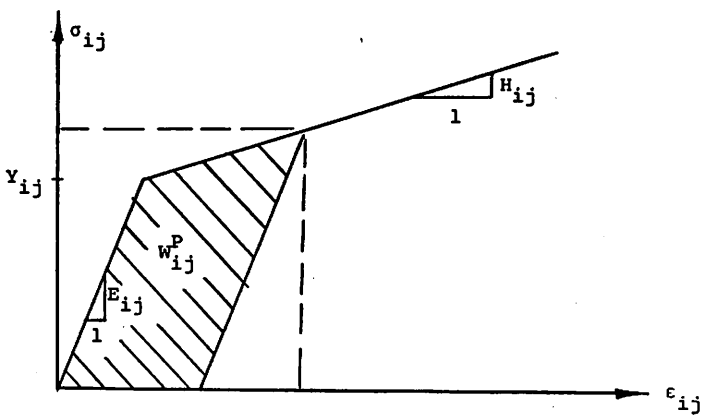

Fig. 1. Bi-Linear Stress-Strain Diagram

then the anisotropic parameters may be expressed in closed form. They are given by

$$\alpha_{ii} = \left[\xi_i + \frac{\eta_i}{\sigma^2}\right]^{-1} \qquad i = r,\theta,z,rz$$

$$\alpha_{ij} = \frac{1}{2}\left(\alpha_{ii} + \alpha_{jj} - \alpha_{kk}\right) \qquad \begin{matrix} i = r,\theta,z \\ j = \theta,z,r \\ k = z,r,\theta \end{matrix}$$

$$\xi_i = \frac{\kappa_i}{\kappa_z}$$

$$\eta_i = Y_i^2 - \xi_i Y_2^2 \qquad i = r,\theta,z,rz$$

$$\frac{1}{\kappa_i} = \frac{1}{H_i} - \frac{1}{E_i}$$

One will notice that $\alpha_{zz} = 1$. The reason being that the z-direction stress-strain diagram was arbitrarily chosen as the equivalent stress-equivalent strain diagram. Consequently, $\xi_z = 1$ and $\eta_z = 0$ making $\alpha_{zz} = 1$.

Equation (2) will now be expressed using matrix nottion, since this form is especially useful in the derivation that follows. We define the stress vector $\{\sigma\}$, the strain vector $\{\varepsilon\}$, and the anisotropic parameter matrix $[\alpha]$ as (the term "vector" will be used instead of "column" matrix and superscript T designates the transpose)

$$\{\sigma\}^T = \{\sigma_r \sigma_z \sigma_\theta \sigma_{rz}\}^T , \qquad \{\varepsilon\}^T = \{\varepsilon_r \varepsilon_z \varepsilon_\theta \gamma_{rz}\}^T \tag{4}$$

$$[\alpha] = \begin{bmatrix} \alpha_{rr} & -\alpha_{zr} & -\alpha_{r\theta} & 0 \\ -\alpha_{zr} & \alpha_{zz} & -\alpha_{\theta z} & 0 \\ -\alpha_{r\theta} & -\alpha_{\theta z} & \alpha_{\theta\theta} & 0 \\ 0 & 0 & 0 & \beta_{rz} \end{bmatrix} \tag{5}$$

The equivalent stress $\bar{\sigma}$ is now defined by [cf. eq. (2)],

$$\bar{\sigma}^2 = \{\sigma\}^T [\alpha] \{\sigma\} \tag{6}$$

The anisotropic parameters α_{ij} given by eq. (3) are valid for $\bar{\sigma} \geq \bar{Y}_o$; where $\bar{Y}_o$ is the initial value of $\bar{Y}$. Their limiting values, i.e., when $\bar{\sigma} = \bar{Y}_o$ are determined by substituting $\bar{Y}_o^2$ for $\bar{\sigma}^2$ in the above mentioned expressions. Since the z-direction stress-strain diagram was chosen as the $\bar{\sigma} - \bar{\varepsilon}$ diagram then $\bar{Y}_o = Y_z$. Substituting Y_z^2 for $\bar{\sigma}^2$ in eq. (3) yields

$$\alpha_{ii} = Y_z^2 / Y_i^2 \qquad i = r,z,\theta,rz \tag{7}$$

These forms are valid for $0 \leq \bar{\sigma} < \bar{Y}_o$ (where $\bar{Y}_o = Y_z$) and are therefore used as the "initial" values of the anisotropic parameters α_{ij}. Once yielding occurs, forms eq. (3) are used.

The Flow Law

Following a development by Prager [Refs. 6 and 7] we derive the flow laws based upon four restrictive conditions, the Conditions of Continuity, Uniqueness, Irreversibility and Consistency. Although Prager originally stated these restrictive conditions for isotropic materials under isothermal loading conditions, he later extended them to apply for non-isothermal loading [Ref.8]. They are further extended here for non-isotropic materials.

The Condition of Consistency is satisfied by noticing that an incremental change in the yield function eq. (1) equals zero, i.e.,

$$\begin{aligned} df &= 2\bar{\sigma}\, d\bar{\sigma} - 2\bar{Y}\, d\bar{Y} = 0 \\ f &= \bar{\sigma}^2 - \bar{Y}^2 = 0 \end{aligned} \tag{8}$$

Therefore, for "active loading," the increase in the equivalent yield stress $\bar{Y}$ (where $\bar{Y} = \bar{Y}_o$ initially) is determined from eq. (8). Before proceeding to the other restrictive conditions, an expression for $\bar{\sigma}d\bar{\sigma}$ and $\bar{Y}d\bar{Y}$ will be drived.

The state variables E_{ij}, H_{ij}, Y_{ij} (cf. Fig. 1) are assumed to be functions of temperature T, i.e.,

$$E_{rr} = E_{rr}(T), \ldots, \qquad k_{rz} = k_{rz}(T)$$

The anisotropic parameter matrix $[\alpha]$ is therefore a function of $\bar{\sigma}$ and T, i.e.,

$$[\alpha] = [\alpha(\bar{\sigma}, T)]$$

Taking the total derivative of eq. (6) yields

$$d(\bar{\sigma}^2) = \frac{\partial(\bar{\sigma}^2)}{\partial\sigma_{ij}} d\sigma_{ij} + \frac{\partial(\bar{\sigma}^2)}{\partial\bar{\sigma}} d\bar{\sigma} + \frac{\partial(\bar{\sigma}^2)}{\partial T} dT \tag{9}$$

Defining

$$\frac{\partial(\ )}{\partial\bar{\sigma}} = (\ )', \qquad \frac{\partial(\ )}{\partial T} = (\dot{\ })$$

$$\Lambda = 1 - \frac{1}{2\bar{\sigma}} \{\sigma\}^T [\alpha']\{\sigma\} \tag{10}$$

$$\{S\} = [\alpha]\{\sigma\}$$

$$\dot{\bar{\sigma}}^2 = \{\sigma\}^T [\dot{\alpha}]\{\sigma\}$$

Then eq. (9) becomes

$$2\bar{\sigma}\, d\bar{\sigma} = \frac{2}{\Lambda} \{S\}^T \{d\sigma\} + \frac{\dot{\bar{\sigma}}^2}{\Lambda} dT \tag{11}$$

The equivalent yield stress $\bar{Y}$ is a function of the plastic work W^P and temperature T. For materials that may be represented in a bi-linear form (see Fig. 1), we have

$$W^P = \frac{1}{2\kappa} (\bar{Y}^2 - \bar{Y}_o^2) \tag{12}$$

Solving for $\bar{Y}^2$ and remembering that $\kappa = \kappa(T)$, $\bar{Y}_o = \bar{Y}_o(T)$, the total derivative of $\bar{Y}^2$ becomes

$$2\bar{Y}\, d\bar{Y} = 2\kappa\, dW^P + 2\dot{\kappa}W^P dT + 2\bar{Y}_o\dot{\bar{Y}}_o dT \tag{13}$$

Substituting for W^P from eq. (12) into eq. (13) and further substitution of eq. (11) and the above into eq. (8) yields

$$df = \frac{2}{\Lambda} \{S\}^T \{d\sigma\} + \left[\frac{\dot{\bar{\sigma}}^2}{\Lambda} - (\bar{Y}^2 - \bar{Y}_o^2) \frac{\dot{\kappa}}{\kappa} - 2\bar{Y}_o\dot{\bar{Y}}_o\right] dT - 2\kappa\, dW^P = 0 \tag{14}$$

Defining

$$dF = \frac{1}{\Lambda} \{S\}^T \{d\sigma\} + \left[\frac{\dot{\bar{\sigma}}^2}{2\Lambda} - \frac{1}{2} (\bar{Y}^2 - \bar{Y}_o^2) \frac{\dot{\kappa}}{\kappa} - \bar{Y}_o\dot{\bar{Y}}_o\right] dT \tag{15}$$

then eq. (14) becomes

$$df = 2dF - 2\kappa\, dW^P = 0 \tag{16}$$

The various loading conditions are expressed by combining the Conditions of Continuity and Irreversibility and eq. (16). They are given by

$$\begin{aligned} &\text{Unloading:} && dW^P = 0, \quad df < 0, \quad \text{therefore} \quad dF < 0 \\ &\text{Neutral Loading:} && dW^P = 0, \quad df = 0, \quad \text{therefore} \quad dF = 0 \\ &\text{Active Loading:} && dW^P > 0, \quad df = 0, \quad \text{therefore} \quad dF > 0 \end{aligned} \tag{17}$$

As may be seen from eqs. (17), all three loading conditions may be expressed by the one quantity, dF. When examining eq. (15), one notices that active loading may occur when either or both $\{d\sigma\}$ and dT make $dF > 0$. Neutral loading occurs when the increase due to $\{d\sigma\}$ is just cancelled by the decrease due to dT or visa-versa. Finally, unloading occurs when $\{d\sigma\}$ and dT make $dF < 0$. Since $d\varepsilon^P_{ij} \neq 0$ (or $dW^P > 0$) for active loading and $d\varepsilon^P_{ij} = 0$ (or $dW^P = 0$) for neutral loading or unloading, the above eqs. (17) suggest that the flow law which satisfies the Condition of Continuity may be expressed by

$$\begin{aligned} \{d\varepsilon^P\} &= \{G\}\, dF \quad && \text{for} \quad f = 0 \\ &= 0 && \text{for} \quad f < 0 \end{aligned} \tag{18}$$

where $\{d\varepsilon^P\}$ is the plastic strain vector and $\{G\}$ is a positive vector. The vector $\{G\}$ is chosen following an argument given by Prager [Ref. 8]. For isothermal changes of state ($dT = 0$), it is generally accepted that

$$\{d\sigma\}^T \{d\varepsilon^P\} > 0$$

for isothermal active loading. This is the Condition of Uniqueness expressed earlier, and may be fulfilled by setting

$$\{G\} = \frac{1}{\Gamma}\{S\} \tag{19}$$

where $\{S\}$ is given by eq. (10) and Γ is a positive invariant of the state variable. Substitution of eq. (19) into eq. (18) yields the flow law in the following form.

$$\begin{aligned} \{d\varepsilon^P\} &= \frac{1}{\Gamma}\{S\}\, dF \quad && \text{for} \quad f = 0 \\ &= 0 && \text{for} \quad f < 0 \end{aligned} \tag{20}$$

The Condition of Irreversibility is automatically satisfied by the form of eq. (20). Using eq. (20), the increment of plastic work is given by

$$dW^P = \{\sigma\}^T \{d\varepsilon^P\} = \frac{1}{\Gamma}\{\sigma\}^T \{S\}\, dF$$

From eqs. (6) and (10), and the above we have

$$dW^P = \left(\frac{\bar{\sigma}^2}{\Gamma}\right) dF \tag{21}$$

The quantity $(\bar{\sigma}^2/\Gamma)$ is always positive and therefore the plastic work increment is directly proportional to the increment dF. Truly it must be, since

eq. (16) yields

$$dW^P = \frac{1}{\kappa} dF \tag{22}$$

for active loading conditions. When comparing eqs. (21) and (22), we see that

$$\Gamma = \kappa\bar{\sigma}^2 \tag{23}$$

Since $\bar{\sigma}^2$ is a positive definite, κ must be positive for Γ to be positive. However, (for $dT = 0$), one can show (cf. Fig. 1),

$$d\bar{\varepsilon}^P = \frac{1}{\kappa} d\bar{\sigma} \tag{24}$$

where

$$\frac{1}{\kappa} = \frac{1}{H} - \frac{1}{E}$$

Since E is always positive, H (shown in Fig. 1) must be positive to ensure κ to be positive. This implies that materials whose stress-train curves increase followed by a decrease (all with increasing $\bar{\varepsilon}$) are not allowed. Combining eq. (23) with (20) yields the final results for the "associated" flow law.

$$\begin{aligned} \{d\varepsilon^P\} &= \frac{1}{\kappa\bar{\sigma}^2} \{S\}\, dF \quad \text{for} \quad f = 0 \\ &= 0 \quad \text{for} \quad f < 0 \end{aligned} \tag{25}$$

The Plasticity Matrix

Substituting for dF from eq. (15) into the flow law eq. (25) yields

$$\{d\varepsilon^P\} = \frac{1}{\kappa\bar{\sigma}^2\Lambda} \{S\}\{S\}^T \{d\sigma\} + \frac{1}{\kappa\bar{\sigma}^2} \left[\frac{\dot{\bar{\sigma}}^2}{2\Lambda} - \frac{1}{2}(\bar{Y}^2 - \bar{Y}_o^2)\frac{\dot{\kappa}}{\kappa} - \bar{Y}_o\dot{\bar{Y}}_o\right]\{S\}\, dT \tag{26}$$

The "plasticity matrix $[D^P]$" and the "thermal plasticity vector $\{\Phi\}$" are defined as

$$\begin{aligned} [D^P] &= \frac{1}{\kappa\bar{\sigma}^2\Lambda}[\Psi] = \frac{1}{\kappa\bar{\sigma}^2\Lambda}\{S\}\{S\}^T \\ \{\Phi\} &= \frac{1}{\kappa\bar{\sigma}^2}\left[\frac{\dot{\bar{\sigma}}^2}{2\Lambda} - \frac{1}{2}(\bar{Y}^2 - \bar{Y}_o^2)\frac{\dot{\kappa}}{\kappa} - \bar{Y}_o\dot{\bar{Y}}_o\right]\{S\} \end{aligned} \tag{27}$$

Combining the definitions eq. (27) with eq. (26) yields

$$\{d\varepsilon^P\} = [D^P]\{d\sigma\} + \{\Phi\}dT \tag{28}$$

Therefore, the plastic strain increment due to a stress increment is given by the "plasticity matrix $[D^P]$", and that due to a temperature increment is given by the "thermal plasticity vector $\{\Phi\}$". They are found by combining eqs. (6), (10), (24), (26), and (27). Expressions for $[\dot{\alpha}]$ and $[\alpha']$ are readily obtained by differentiating eqs. (3) and (7).

Derivation of the Elasticity Matrix

For orthotropic materials, mechanical strains are related to stres and thermal strains by Hooke's law given in the following form

$$\{\varepsilon^M\} = [D^E]\{\sigma\} + \{\alpha\}(T - T_o) \tag{29}$$

where the coefficients D^E_{ij} are given in engineering notation by

$$D_{ii} = \frac{1}{E_i}\ , \quad D_{ij} = \frac{-\nu_{ij}}{E_i} = \frac{-\nu_{ji}}{E_j} \qquad \begin{matrix} i = 1,2,3 \\ j = 2,3,1 \end{matrix}$$

$$D_{44} = \frac{1}{G_{rz}}\ , \quad D_{i4} = 0 \qquad (1 = r,\ 2 = \theta,\ 3 = z) \tag{30}$$

and where T_o is the reference temperature. Take special care not to confuse the linear expansion coefficient "vector" $\{\alpha\}$ defined by

$$\{\alpha\}^T = \{\alpha_r\ \alpha_z\ \alpha_\theta\ 0\}^T \tag{31}$$

with the anisotropic parameter <u>matrix</u> $[\alpha]$. In the plastic range, we are interested in strain increments. Differentiating eq. (29) and remembering $(\dot{}) = \partial(\ )/\partial T$ yields

$$\{d\varepsilon^E\} = [D^E]\{d\sigma\} + [\dot{D}^E]\{\sigma\} + \{\dot{\alpha}\}(T - T_o) + \{\alpha\}\ dT$$

Defining a "thermal elasticity vector $\{\bar{\alpha}\}$" by

$$\{\bar{\alpha}\} = \{\alpha\} + [\dot{D}^E]\{\sigma\} + \{\dot{\alpha}\}(T - T_o)$$

the above incremental equation becomes

$$\{d\varepsilon^E\} = [D^E]\{d\sigma\} + \{\bar{\alpha}\}\ dT \tag{32}$$

The elastic strain increment due to a stress increment is given by the "elasticity matrix $[D^E]$" and that due to a temperature increment is given by the "thermal elasticity vector $\{\bar{\alpha}\}$". Expressions $[\dot{D}^E]$ and $\{\dot{\alpha}\}$ are again easily derived by differentiation.

<u>Incremental-Variable Stiffness Method</u>

By adding the elastic strain increment given by eq. (32) to the plastic strain increment given by eq. (28), the total strain increment becomes

$$\{d\varepsilon\} = ([D^E] + [D^P])\{d\sigma\} + (\{\bar{\alpha}\} + \{\Phi\})\ dT \tag{33}$$

Inverting the above relation yields

$$\{d\varepsilon\} = [C^{EP}]\{d\varepsilon\} - \{d\tau\} \tag{34a}$$

where

$$[C^{EP}(\sigma,\varepsilon^P)] = ([D^E] + [D^P])^{-1}$$

$$\{d\tau\} = [C^{EP}](\{\bar{\alpha}\} + \{\Phi\})\ dT \tag{34b}$$

$[C^{EP}]$ is the "variable elastic-plastic coefficient matrix" and $\{d\tau\}$ is the thermal stress matrix arising from dT. Applying the variational principles used by the finite element method to the above relationship yields

$$\{dF\} = [K]\{du\} \tag{35}$$

where $\{dF\}$, the incremental force vector, contains both $\{d\sigma\}$ and $\{d\tau\}$, $[K]$ is the variable stiffness matrix, and $\{du\}$ is the incremental displacement vector. As can be seen in this relation $[K]$ is a function of the current stress and plastic strain, and therefore a separate problem must be solved in each increment. Two procedures are available, a direct incremental approach and an iterative-incremental approach. The algorithm for the direct incremental approach is

$$\{dF_m\} = [K_{m-1}]\{du_m\} \tag{36}$$

A modification of this direct incremental approach would be to use the "mid-point rule". This would require two iterations per increment, as illustrated in the following steps.

(a) $[K_{m-1}]\{du_m\} = \{dF_m\}$

(b) $\{u_{m+1/2}\} = \{u_m\} + \frac{1}{2}\{du_m\}$

$\{F_{m+1/2}\} = \{F_m\} + \frac{1}{2}\{dF_m\}$

(c) $\{u_{m+1/2}\}, \{f_{m+1/2}\} \rightarrow [K_{m-1/2}]$

(d) $[K_{m-1/2}]\{du_m\} = \{dF_m\}$

where $[K_{m-1/2}]$ is the value of the variable stiffness matrix at the "mid-point" between $\{u_m\}$ and $\{u_m + du_m\}$. This mid-point rule uses the average variable stiffness matrix, thereby improving accuracy of the procedure. The disadvantage is that the variable stiffness matrix $[K]$ must be calculated twice in each increment, which is time consuming. By far, the most accurate of all these procedures is the incremental-iterative approach of the variable stiffness method. Here the non-linear problem

$$[K(F,u)]\{du\} = \{dF\} \tag{37}$$

is solved iteratively in each increment, thereby minimizing errors and obtaining the highest degree of accuracy for this incremental method of solution. To obtain the exact solution, the increment size must be indefinitely reduced to zero.

Since the problem is being solved on a digital computer, questions of numerical errors become important for such a large number of calculations. All of these important questions on accuracy should be answered to make any elastic-plastic solution meaningful.

The above incremental constitutive equations were incorporated into the OASIS finite element code which was developed to solve plasticity problems for bodies of revolution (see Ref. 5). A comprehensive description of the formulation is given in Ref. 5. The solution procedure is presented in flow chart form, and is given in Fig. 2. The incremental solution is found

following a technique used by Yamada, Yoshimura and Sukurai [Ref. 9]. The size of the incremental step is iteratively determined such that the most highly stressed elastic element which is actively loading (increasing in stress level) just reaches a plastic state. The iterative procedure is required since both the incremental thermal loads and the stiffnesses of the elements are functions of the instantaneous temperature loads. In addition to this iterative procedure, there is a provision to limit the incremental step size to some predetermined fraction of the total load size. This iterative procedure determines the ratio factor "r" such that for the highest stressed elastic element,

$$r \cdot d\bar{\sigma} = \bar{Y} - \bar{\sigma} = \Delta\bar{\sigma} \tag{38}$$

which will cause that element to just yield. Using Newton's iteration method to determine "r", then the i+1 estimate of r_i is given by

$$r_{i+1} = r_i - \frac{f(r_i)}{f'(r_i)} \tag{39}$$

where the yield function $f(r_i)$ is given by

$$f(r_i) = \bar{\sigma}_i^2 - \bar{Y}_i^2 \tag{40a}$$

with

$$\bar{\sigma}_i^2 = \{\sigma\}_i^T [\alpha(\bar{\sigma}_i, T_i)]\{\sigma\}_i \ , \qquad \bar{Y}_i = \bar{Y}(T_i)$$
$$\{\sigma\}_i = \{\sigma + r_i d\sigma\} \ , \qquad T_i = T + r_i dT \tag{40b}$$

and

$$f'(r_i) = \frac{\partial}{\partial r} f(r_i) = 2\bar{\sigma}_i \frac{\partial \bar{\sigma}_i}{\partial r} - 2\bar{Y}_i \frac{\partial \bar{Y}_i}{\partial r} \tag{41a}$$

with the linearizations

$$\frac{\partial \bar{\sigma}_i}{\partial r} = d\bar{\sigma}_i \ , \qquad \frac{\partial \bar{Y}_i}{\partial r} = d\bar{Y}_i \tag{41b}$$

Assessment of the Affect of Material Orthotropy

To assess the effect that orthotropic material properties play in the present orthotropic thermal plasticity theory, two similar problems were solved, one being isotropic, the other orthotropic. Plane strain hollow cylinders loaded by a temperature distribution were chosen for the comparison. The material properties were taken to be independent of temperature, and orthotropy is introduced by assuming the yield stress in the hoop direction is different from the value for the radial and axial directions. Thus, the material has a plane of isotropy, the radial/axial plane. The isotropic material properties are given in Fig. 3 where E = Young's modulus, ν = Poisson's ratio, α = coefficient of linear thermal expansion, Y = yield stress in tension and k = the yield stress in shear. The assumed temperature distribution is given by

$$T(r) = \frac{T_o a}{b - a}\left(\frac{b}{r} - 1\right) \qquad a \leq r \leq b \tag{42}$$

where T_o (= 800°F) is the temperature at the inside radius, r = a. The finite element model used consisted of 20 ring elements, extending from the inside radius r = a to the outside radius r = b.

The non-dimensional stresses σ_i/Y , i = r,θ,z compromising the elastic-plastic solution for the orthotropic hollow plane strain cylinders loaded by the above temperature distribution are given in Fig. 3 for the two cases $Y_\theta = Y$ and $Y_\theta = 0.5Y$ (shown by solid lines). In addition, the elastic solution, which is independent of the yield stresses and therefore applies to both solutions, are shown by dashed lines. These two solutions provide an important illustration of the effects of inelastic orthotropy in materials.

For the isotropic case ($Y_\theta = Y$), plasticity initiated on the inside surface of the cylinder r = a and spread outward under the specified thermal loading. Conversely, when $Y_\theta = 0.5Y$, plasticity initiated on the outside surface of the cylinder r = b and spread inward. Consequently, the elastic-plastic state is strongly dependent on the degree of orthotropy in the hoop direction. It is seen that the character of the orthotropic inelastic behavior can be quite different from that of an isotropic material under similar conditions.

Assessment of Certain Effects Arising from Temperature Dependence of Material Properties

The incremental, orthotropic elastic-plastic-thermal constitutive equations may be restated here in the following form (cf. eqs. (28), (32), and (33))

$$\{d\varepsilon\} = ([D^E] + [D^P])\{d\sigma\} + \{\alpha\}dT + (\{\phi\} + \{\dot{\alpha}\}(T - T_o) + [\dot{D}^E]\{\sigma\})dT \tag{43}$$

The incremental strain due to a temperature increment dT has been divided into two parts. The first part is simply the elastic thermal strain in incremental form. The second part contains three terms, all of which are attributable to temperature dependence of the material properties; i.e., these terms represent incremental strain due to the "rate of change" of the material properties with respect to temperature. They will be referred to herein as "temperature-rate" terms. To ascertain the effect that these temperature-rate terms have on elastic-plastic-thermal deformations, a plane strain hollow cylinder problem was solved both including and neglecting the influence of these terms. The material properties are taken to the orthotropic and temperature dependent. It is assumed that all of the material properties (with the exception of Poisson's ratio which is assumed constant) increase in value by 10 percent for every 100°F temperature rise. This may be expressed by the following relation: $f(T) = f_o(1 + 0.001T)$ where f represents a material property. The material properties are isotropic, with the following exception: orthotropy is introduced by assuming that the hoop yield stress $Y_\theta = 1.3Y$ (where Y is the

isotropic value). The properties at zero temperature are given in Fig. 4. The temperature loading is taken as the steady state distribution

$$T(r) = T_o \frac{\ell n(r/a)}{\ell n(b/a)} \quad . \quad a \leq r \leq b$$

where $T_o = 250^oF$ is the steady state temperature of the outside surface $r = b$. The finite element model consists of 20 elements, extending from $r = a$ to $r = b$.

The problem was solved with the OASIS code using two different methods. In the first method, all of the effects of material property variation with respect to temperature were retained, and the results are shown by solid lines in Fig. 4. The second method of solution neglected all of the "temperature-rate" terms but retained all other effects of property temperature dependence. These latter results are shown by dashed lines in Fig. 4 (where k_o is the shear yield stress and E_o is Young's modulus at zero temperature). The maximum differences occur in the neighborhood of the outside surface $r = b$. The stresses are 11 percent to 13 percent low and the strains are 14 percent to 16 percent low when the temperature-rate terms are neglected. This error, is, of course, dependent upon how the material properties vary with temperature. Yielding for both solutions first occurred for an outside surface temperature $T_o = 120.7^oF$. The final surface temperature was $T_o = 250.0^oF$. Hence, the temperature difference of 129.3^oF produced a 12.93 percent change in material properties (at the outside surface $r = b$) from initiation of plastic flow to the final elastic-plastic state. For this particular problem, the error introduced by neglecting the above rate terms is of the same magnitude as the material property temperature dependence.

This example has clearly shown that for materials with appreciable temperature dependent material properties, the correct elastic-plastic-thermal incremental method of solution must include the temperature-rate terms given in eq. (43).

Graphite Investigations

Graphite investigations are presented in this section for two different comparisons; the first compares incremental plasticity theory with deformation plasticity theory, the second compares actual stress-strain curve solutions with bi-linear stress-strain curve solutions.

In the first comparison, bi-linear stress-strain curves obtained from the actual stress-strain curves by a "least-squares" best fit procedure are used. A typical example of such a bi-linear curve is shown in Figure 6a for ATJ-S (Tension, With Grain) @ 4500^oF. In the second comparison, both bi-linear and actual stress-strain curve data is used. Figure 5 contains all of the bi-linear data for both tension and compression loading and with and across grain directions.

A problem was selected to illustrate the differences between solutions obtained by deformation theory and by incremental theory of plasticity. A

hollow cylinder was investigated loaded by a temperature distribution shown in Fig. 6b ($\tau = 0.10$). The elastic-plastic-thermal solution to this problem was obtained by both the incremental theory code (OASIS) and a deformation theory code (DOASIS).*

The stress and strain components obtained by the above two methods of solution are shown in Fig. 7. The dashed curves are the incremental (OASIS code) results and the solid curves the deformation theory (DOASIS code) results. Significant differences exist between these two solutions:

- In the incremental solution, the final state is elastic from r/a = 1.0 to 1.65, plastic from r/a = 1.65 to 1.85 and elastically unloaded from r/a = 1.85 to 2.00. To indicate this unloading from a plastic state, the maximum stress level reached during the incremental solution is also shown in Fig. 7 for elements in the region r/a = 1.85 → 2.00. This maximum stress envelope is indicated only for the axial (σ_z) component of stress.
- In the deformation solution, the final state is elastic from r/a = 1.00 to 1.65 and plastic from r/a = 1.65 to 2.00.
- The predicted elastic and plastic strains are completely different in the inelastic region. Since unloading occurred from r/a = 1.85 to r/a = 2.00 in the incremental solution, only small plastic strains were developed. Conversely, large plastic strains were predicted in the deformation theory solution.
- The total maximum equivalent strains, i.e., $\bar{\varepsilon} = [2/3\{(\varepsilon_r - \varepsilon_\theta)^2 + (\varepsilon_\theta - \varepsilon_z)^2 + (\varepsilon_z - \varepsilon_r)^2\}]^{\frac{1}{2}}$ were completely different. The maximum equivalent strain in the deformation theory results occurred at r/a = 2.0 and had a value of $\bar{\varepsilon}_{max} = 0.02229$; the corresponding maximum equivalent strain predicted for r/a = 2.0 by the incremental theory was $\bar{\varepsilon} = 0.00857$ (notice that $\bar{\varepsilon}_{max}$ did not occur at r/a = 2.0 for the incremental theory results). Hence, completely erroneous conclusions could be drawn from the deformation theory results for this problem if the failure criterion were based upon the maximum equivalent strain.

Both of these solutions were obtained for a monotonically increasing thermal load. Hence, an important unloading phenomenon was observed. The unloading of a portion of the structure under monotonically increasing thermal load apparently resulted from the temperature dependence of the material mechanical properties.

Such path dependent phenomena cannot be predicted with a deformation plasticity code because arbitrary load histories are not accounted for. In general, an incremental formulation is required to correctly and reliably

*DOASIS is a finite element code similar to OASIS with deformation plasticity being the method of solution. Consequently, load path dependence is neglected.

predict detailed thermostructural response when load path dependent effects, such as temperature dependent inelastic behavior, are important. The deformation plasticity theory code is a useful tool for rapidly obtaining approximate answers for engineering design, but the validity of such computational results can only be assessed by an incremental analysis.

Comparison of Results Based on Actual Stress-Strain Data and on Best-Fit Bi-Linear Representations

Incremental solutions were generated for thermal loading of hollow graphite cylinders using actual stress-strain data and also best-fit bi-linear representations. These solutions are compared in order to examine the adequacy of thermostructural predictions based on bi-linear approximations to actual stress-strain data. The same plane strain hollow cylinder with the temperature loading (τ = 0.10) in Fig. 6b analyzed above is used in this comparison.

The stress and strain results are shown in Fig. 8. The results for the actual stress-strain data are represented by solid lines; results for the bi-linear stress-strain curves are represented by dashed curves. Comparison of stresses, elastic strains and plastic strains for this thermal loading reveals that all three agree quite well, with the axial (z) components showing the largest differences. For this case the magnitude of the plastic strains is considerably less than the corresponding elastic strains. The reason for this is that with thermal loading, the straining in the material is caused by differential thermal expansion ($\alpha \Delta T$), which in this case was only slightly larger than the elastic strains. Consequently, only relatively small plastic strains developed.

Further Areas of Research

The above analysis was for a mono-modulus material, i.e., the same properties in tension and compression for both the elastic and plastic regimes. For graphites, this approximation is unacceptable as may be seen when viewing Fig. 5. Both the elastic properties (Young's modulii E_i) and plastic properties (yield stresses $\bar{Y}_i$ and tangent modulii H_i) are considerably different. Recent work by Ambartsumyar [Ref. 10] and Jones [Ref. 11] describes a multi-modulus model for the thermal-elastic response. The next logical step is to include the thermal-plastic response of multi-modulus materials. In addition, plastic volume changes have been observed in tests and should be included in the plastic model. The author is presently working in this area. The largest difficulty encountered by the author is finding independent tests which will yield the necessary material parameters. The analysis is only as sufficient as the accuracy of the characterization.

Acknowledgement

The majority of this work was performed under United States Air Force Contract No. F33615-69-C-1627 monitored by the Air Force Materials Laboratory, WPAFB, Dayton, Ohio. The author would like to thank them for their support.

REFERENCES

[1] Personal communication with Colt Pears, Southern Research Institute, Birmingham, Alabama.

[2] HILL, R., The Mathematical Theory of Plasticity, Oxford University Press, Oxford, 1950.

[3] HU, L. W., MARIN, J., "Anisotropic Loading Functions for Combined Stresses in the Plastic Range," Journal of Applied Mechanics, Vol. 22, March 1955, pp. 77-85.

[4] JENSEN, W. R., FALBY, W. E., PRINCE, N., "Matrix Analysis Methods for Anisotropic Inelastic Structures," AFFDL-TR-650220, Air Force Flight Dynamic Laboratory, Wright-Patterson Air Force Base, Ohio, April 1966.

[5] WEILER, F. C., "Elastic-Plastic-Thermal Analysis of Anisotropic Bodies of Revolution by the Finite Element Method," report to be published by Aerotherm Corporation, Mountain View, California, 1971.

[6] PRAGER, W., "The Stress-Strain Laws of the Mathematical Theory of Plasticity - A Survey of Recent Progress," Journal of Applied Mechanics, Vol. 15, September 1948, pp. 226-233.

[7] PRAGER, W., "Recent Developments in the Mathematical Theory of Plasticity," Journal of Applied Physics, Vol. 20, March 1949, pp. 235-241.

[8] PRAGER, W., "Non-Isothermal Plastic Deformation," Koninklijke Nederlandse Akademie Van Wetenschappen, Proceedings (Series B), Vol. 61, January 1958, pp. 176-182.

[9] YAMADA, Y., YOSHIMURA, N., SAKURAI, T., "Plastic Stress-Strain Matrix and Its Application for the Solution of Elastic-Plastic Problems by the Finite Element Method," International Journal of the Mechanical Sciences, Vol. 10, 1968, pp. 343-354.

[10] AMBARTSUMYAN, S. A., "Basic Equations and Relations in the Theory of Elasticity of Anisotropic Bodies with Differing Modulii in Tension and Compression," Inzhenernyi Zhurnal, Mekhanika, tverdogo tela, No. 3, 1969, pp. 51-61.

[11] JONES, R. M., "Buckling of Circular Cylindrical Shells with Different Modulii in Tension and Compression," AIAA Journal, Vol. 9, No. 1, January 1971, pp. 53-61.

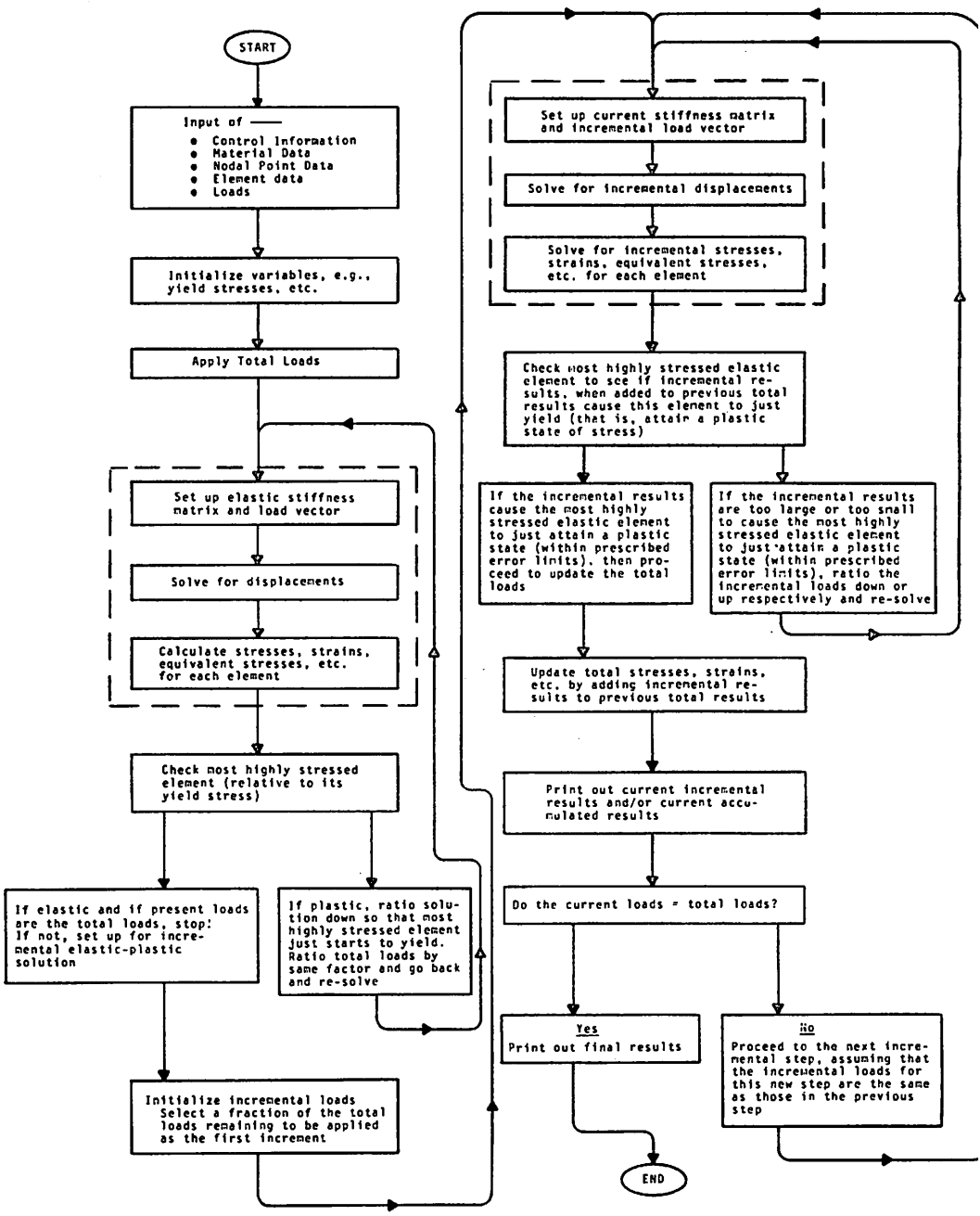

Fig. 2 Flow Chart of the OASIS Code

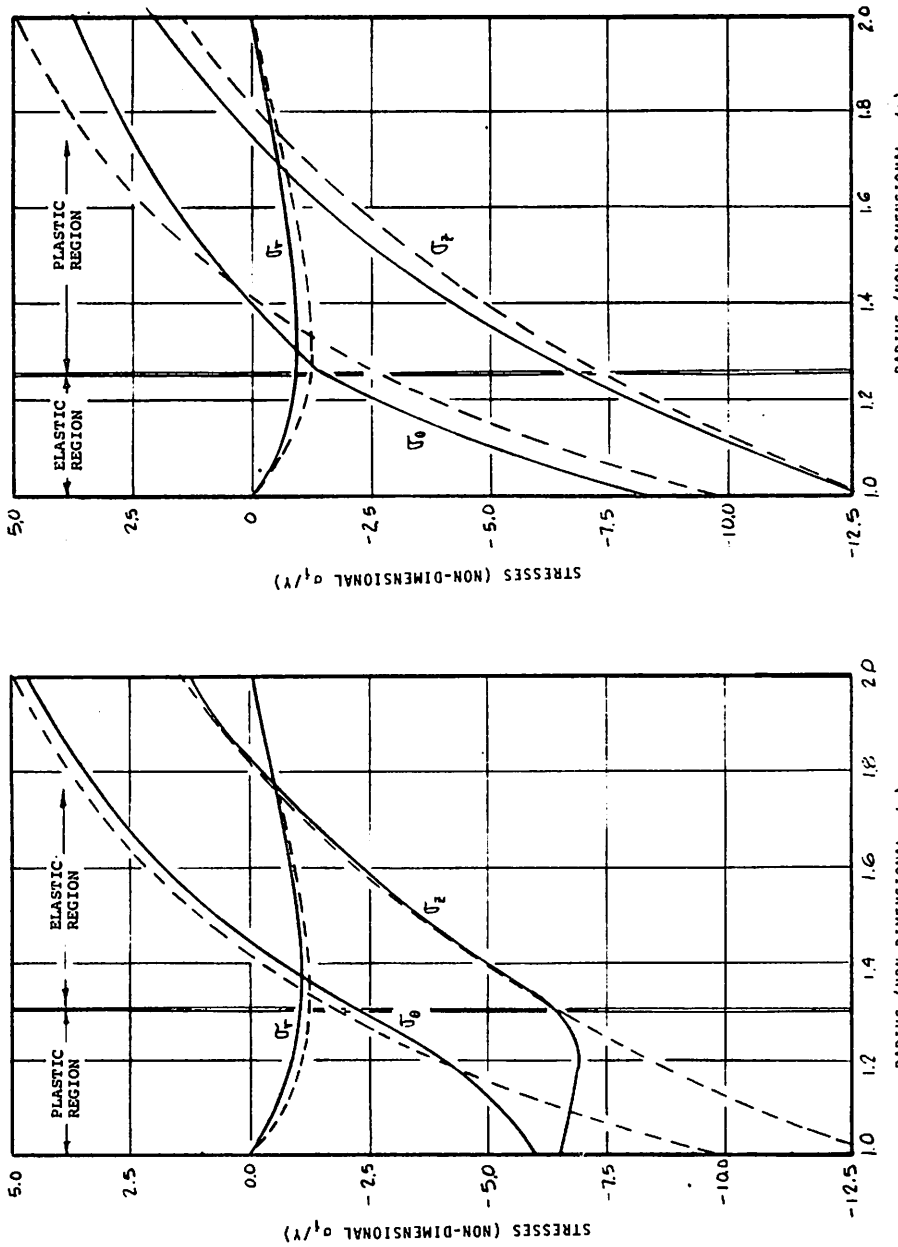

Fig. 3 Comparison of Inelastic Response of Hollow Plane Strain Cylinders ($E/Y = 208.0$, $Y/k = \sqrt{3}$, $\nu = 0.30$, $\alpha = 12.5 * 10^{-6}$)

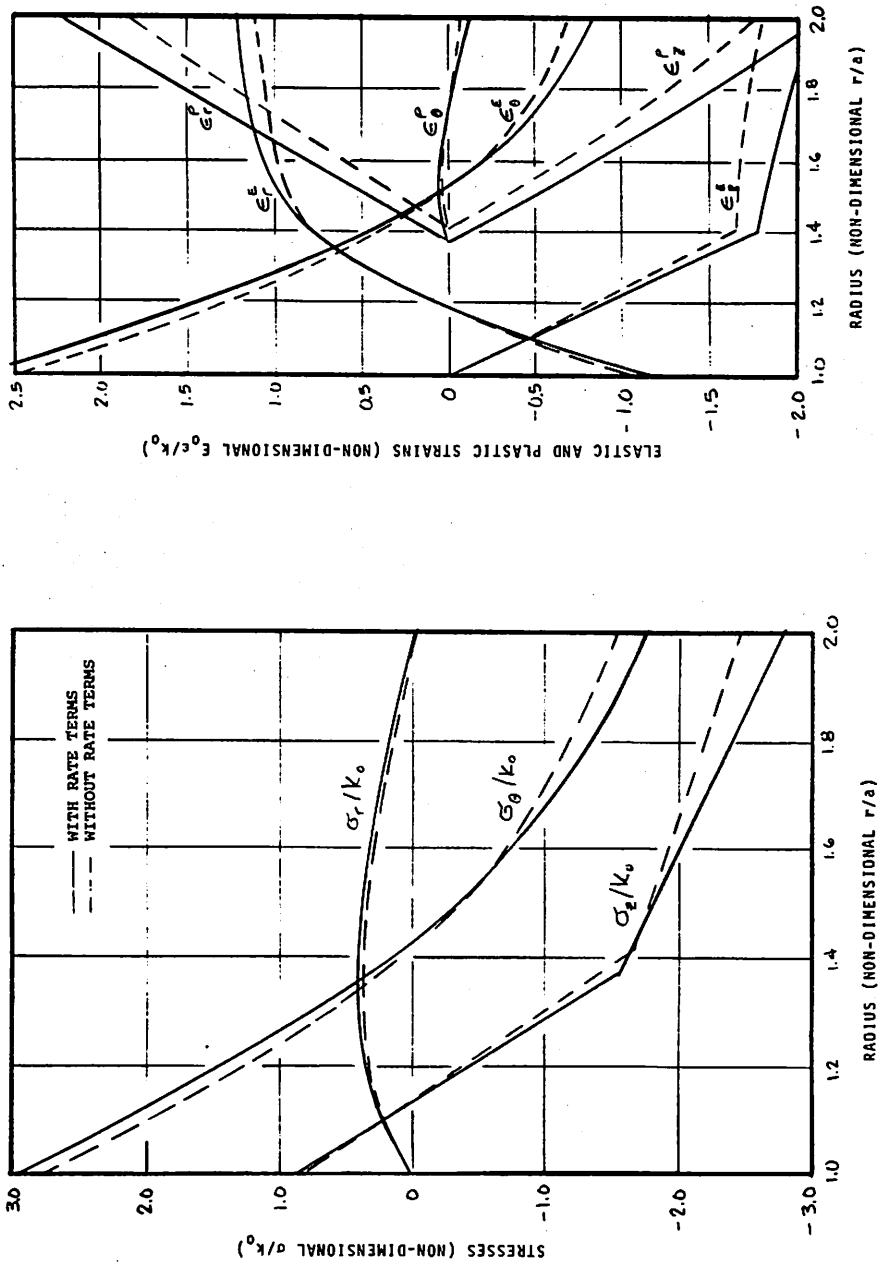

Fig. 4 Assessment of Temperature Rate Terms in Incremental Constitutive Equations (@ T = 0, E_o/k_o = 1000.0, ν = 0.3, H_o/E_o = 0.12162, α_o = 12.5 10^{-6}, $k_o = Y_o/\sqrt{3}$

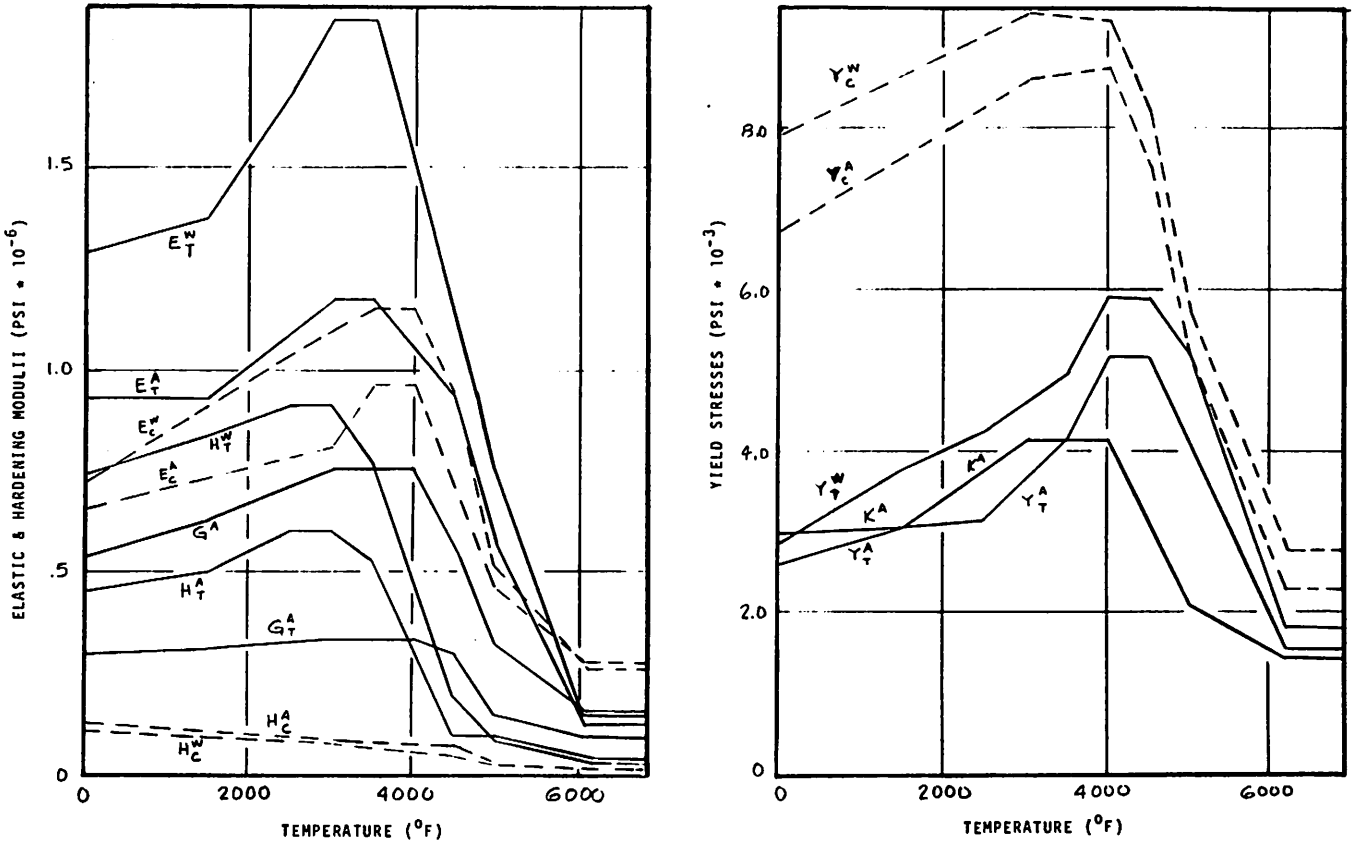

Fig. 5 ATJ-S Graphite Mechanical Properties (Superscripts: w = with grain, A = across grain; subscripts: C = compression, T = tension)

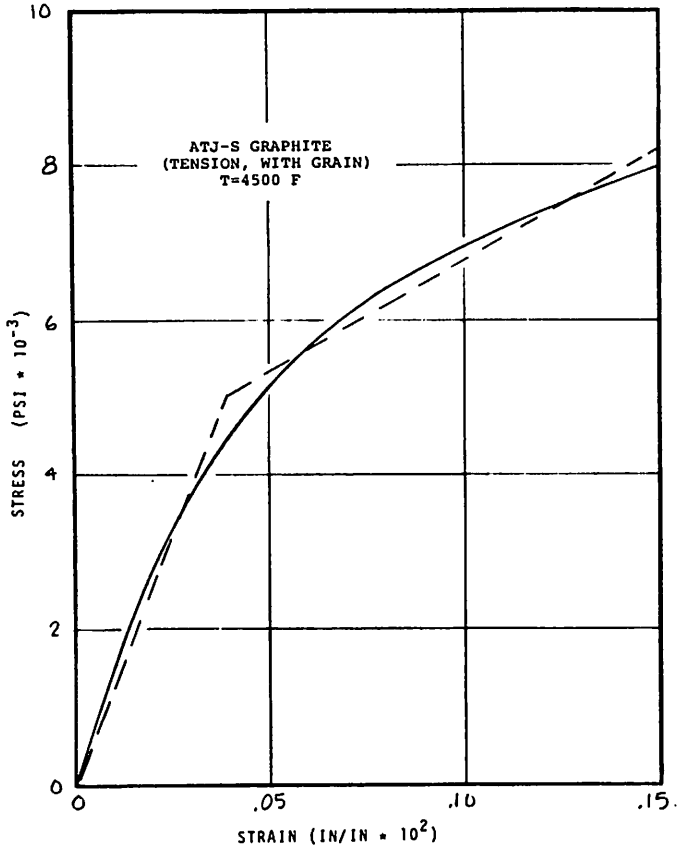

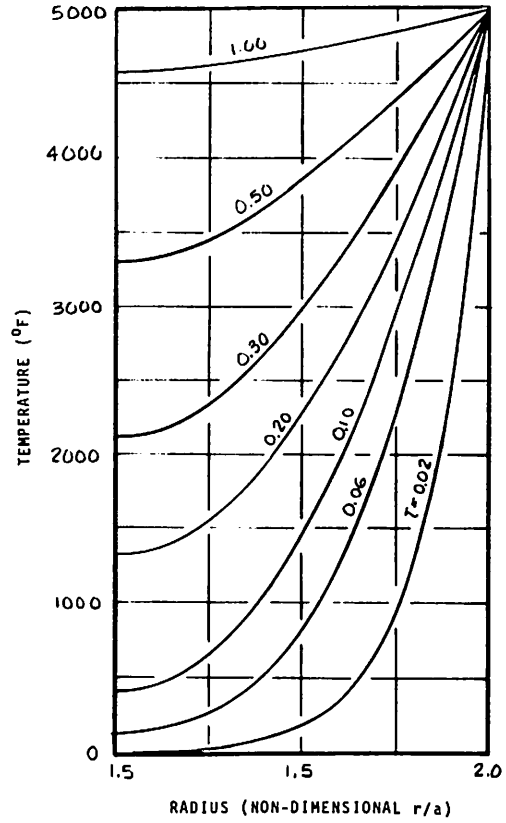

Fig. 6 (a) Actual and Bi-Linear Stress-Strain Curves of ATJ-S Graphite
(b) Temperature Distributions in Hollow Graphite Cylinder. For Various Times τ

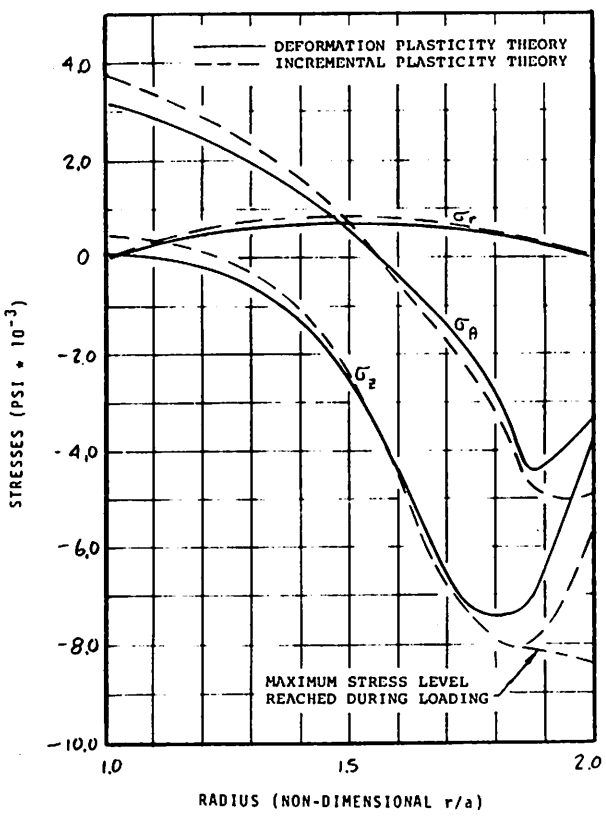

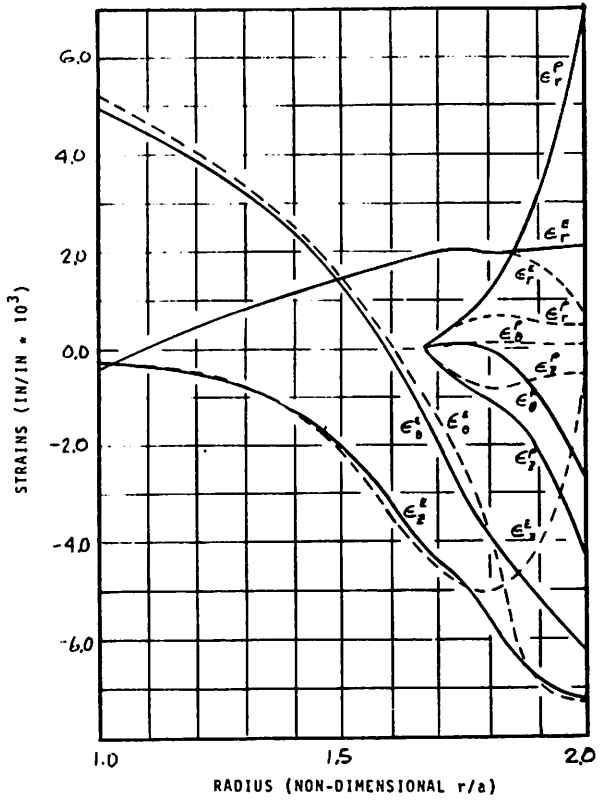

Fig. 7 Stresses and Strains in a Thermally Loaded Hollow, Plane Strain Graphite Cylinder Obtained by Both Incremental and Deformation Plasticity Theories

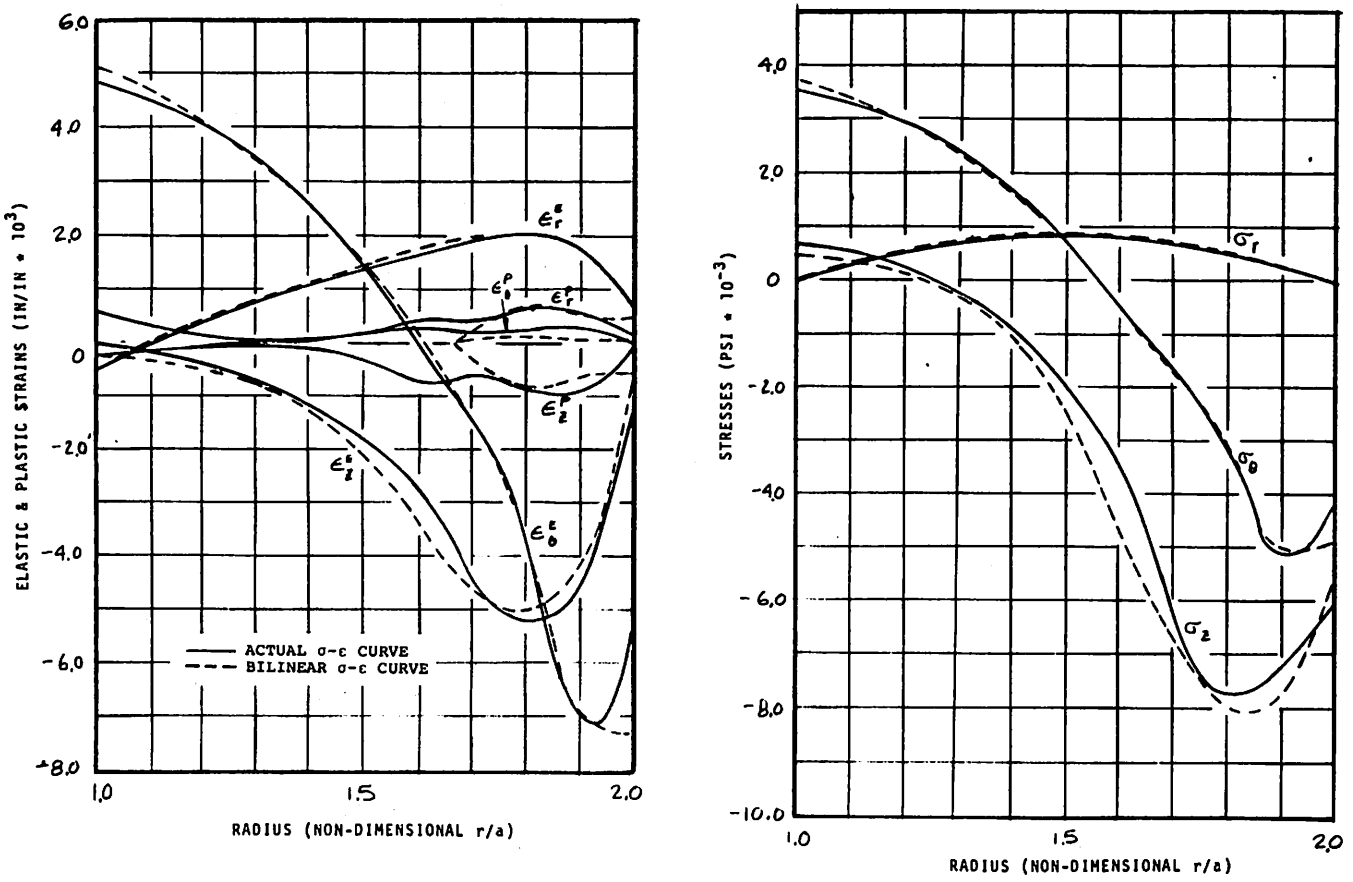

Fig. 8 Stresses and Strains in a Thermally Loaded Hollow, Plane Strain Graphite Cylinder Obtained by Using Both Actual and Bi-Linear Stress-Strain Curves

DISCUSSION

Q J. H. ARGYRIS, U. K. /Germany

1. Congratulations on an excellent piece of work. As you pointed out yourself the contribution due to temperature in the plastic strain expression was also mentioned in our lecture by Dr. Willam.

2. One is astonished in today's computer age it should be necessary to justify the incremental as against the total strain rule in plasticity. This is surely a relique from the analytical days.

A F. C. WEILER, U. S. A.

1. I did not have a chance to see the details of how Dr. Willam incorporates this thermal plastic strain term for orthotropic or even anisotropic materials. Many people present a general formulation, showing that the plastic strain vector is normal to the yield surface, etc. Very few have included the terms of the plastic strain increment due to the temperature increment. I did not have a chance to read Dr. Willam's paper before the conference, but after listening to his talk, I think he also includes this term. My paper presents these terms in an explicit form, i. e., formulas which can be used for a mono-modulus, orthotropic material which has a yield surface which is independent of hydrostatic pressure and hardens isotropically. Unfortunately, I have not seen other explicit expressions in the literature.

2. Unfortunately, some people still insist on using a total strain theory, and so one must show them, with examples as I have presented, that this technique is invalid, and should not be used.